DOI 10.5012/bkcs.2010.31.5.1177

Gold Nanoparticles Coated with Gd-Chelate as a Potential CT/MRI Bimodal Contrast Agent

Nasiruzzaman Sk Md.,[†] Hee-Kyung Kim,[‡] Ji-Ae Park,[§] Yongmin Chang,[‡,#,*] and Tae-Jeong Kim[†,*]

[†]*Department of Applied Chemistry, Kyungpook National University, Daegu 702-701, Korea. [*]E-mail: tjkim@knu.ac.kr*
[‡]*Department of Medical & Biological Engineering, Kyungpook National University, Daegu 702-701 Korea [*]E-mail: ychang@knu.ac.kr*
[§]*Laboratory of Nuclear Medicine Research Molecular Imaging Center, Korea Institute of Radiological Medical Science, Seoul 139-706 Korea*
[#]*Department of Diagnostic Radiology & Molecular Medicine, Kyungpook National University, Daegu 702-701, Korea*
Received September 8, 2009, Accepted February 26, 2010

The synthesis and characterization of gold nanoparticles coated by Gd-chelate (GdL@Au) is described, where L is a conjugate of DTPA (DTPA = diethylenetriamine-*N*,*N*,*N*',*N*'',*N*''-pentaacetic acid) and 4-aminothiophenol. These particles are obtained by the replacement of citrate from the gold nanoparticle surfaces with gadolinium chelate (GdL). The average size of GdL@Au is 12 nm with a loading of GdL reaching up to 1.4×10^3 per particles, and they demonstrate very high $r1$ relaxivity ($\sim 10^4$ $mM^{-1}s^{-1}$) and the $r1$ relaxivity per [Gd] is as high as 10 $mM^{-1}s^{-1}$. Here, we also describe the use of bimodality of this contrast agent (CA) as a highly efficient CT contrast agent based on gold nanoparticles (GNPs) that overcome the limitations of iodine based contrast agent. The MTT assay performed on this CAs reveals the cytotoxicity as low as that for Omniscan® in the concentration range required to obtain intensity enhancement in the *in vivo* MRI study

Key Words: MRI, MRI CA, Bimodality, Gd-DTPA, MRI-CT

Introduction

A rapidly growing versatile research area in experimental diagnostic radiology is molecular imaging, aiming to image biological processes by shortening the T1-relaxation times of the water proton.[1-2] Magnetic resonance imaging (MRI) has become one of the most important and easily available imaging modalities in clinics because of its fast scan times, its capacity to produce excellent quality and high-resolution images, and because there is no need for radiochemicals. Such usability implies adequate pharmacokinetic properties and low levels of nonspecific accumulation in the body. In recent, many research groups emphasize the development of nanoparticles as contrast agents for medical imaging since relaxivities are much higher than those of clinically approved Gd-chelates[3] and they have a longer vascular half-life than molecular contrast agents. A representative example includes water-soluble apoferritin-encapsulated GdNPs with T1 and T2 relaxivities much higher than those of classical Gd (III)-complexes (10 - 25 and 70 times, respectively).[4] Another versatile research area has been explored toward the development of multifunctional contrast agents (CAs) for use across multiple imaging modalities such as PET/MRI, PET/CT, SPECT/CT etc.[5] In the clinics, correlative studies using combinations of this imaging methods, are often performed on the patient simultaneously which is cost effective and time saving. In line with this effort, various paramagnetic nanomaterials with multifunctional modality have been emerged. For instance, hybrid nanoparticles consisting of $Gd_2O(CO_3)_2 \cdot H_2O$/silica/gold and gold nanoparticles coated with GdL have been reported as bifunctional agents for MRI/photothermal destruction of cancer cells.[6]

In contrast to the availability of such diverse multifunctional imaging modalities as mentioned above, MR/CT bimodality has rarely been explored although the two techniques are separately applied to the same patient to improve the accuracy of diagnosis or assess the efficacy of treatment routines. CT, which is one of the most useful diagnostic tools in terms of frequency of use and cost, has high spatial resolution and good hard tissue contrast. Current CAs for CT are based on iodinated small molecules because, among nonmetal atoms, iodine has a high X-ray absorption coefficient.[7] Iodinated compounds, however, allow only very short imaging times due to rapid clearance by the kidney, which can also cause them to have renal toxicity. In this regard, it is worth noting that novel nanoparticle-based CT CAs have recently emerged to overcome the shortcomings of iodine-based agents. Gold nanoparticles (AuNPs), for instance, have demonstrated a great potential as an excellent substitute for iodine.[8] The employment of AuNPs in CT offer some unique advantages in that gold has a higher X-ray absorption coefficient than iodine (5.16 and 1.94 cm^2/g, respectively, at 100 keV) and at the same time biocompatible and nontoxic *in vivo*. Furthermore, an additional advantage of AuNPs comes from the fact that facile surface modification may lead to the formation of various functionalities applicable to multiple imaging modalities such as MRI and CT. In this regard, it is worth to mention that Roux has recently demonstrated for the first time that AuNPs coated with paramagnetic Gd(DTDTPA), Gd(DTDTPA)@Au, is an attractive bimodal MRI/CT CA. The study reveals that Gd (DTDTPA)@Au may be in many respects a substitute for commercially available, low molecular weight Gd(III)-based MRI CAs.[9]

Yet, considering the fact that most of MRI CAs currently on the market are extracelluar and with low relaxivities, development of bimodal MRI/CT CAs with high relaxivity as well as

high X-ray attenuation is desirable. Intrigued by the work of Roux and motivated by our continued effort to develop a new class of bifunctional MRI/CT CAs with high relaxivity and high CT contrast,[10] herein we report the synthesis, relaxivity and their X-ray attenuation properties of AuNPs coated with Gd-complex of DTPA-bis(amide) conjugate of 4-aminothiophenol, GdL@Au.

Experimental Section

Materials. All reactions were carried out under an atmosphere of dinitrogen using the standard Schlenk techniques. Solvents were purified and dried using standard procedures. Diethylenetriamine-*N*,*N*,*N*',*N*'',*N*''-pentaacetic acid (DTPA) and 4-aminothiophenol obtained from TCI and used without further purification. The *N*,*N*''-bis(anhydride) of DTPA was prepared according to the literature methods.[1] All other commercial reagents were purchased from Aldrich and used as received unless otherwise stated. Deionized water was used for all experiments.

Synthesis of DTPA-bis(amide) of 4-Aminothiophenol (L). To a suspension of DTPA-bis(anhydride) (0.71 g, 2 mmol) in DMF (15 mL) was added 4-aminothiophenol (0.37 g, 4 mmol). The mixture was stirred at 65 °C for 6 h, after which the solvent was removed under reduced pressure, and the residue was taken up in methanol (10 mL). The solution was passed through a short silica gel column with methanol as an eluent. An off-white solid was obtained after removal of the solvent under vacuo at 50 °C for 8 h. Yield 0.87 g (81%). ^{1}H [DMSO-d_6, 400 MHz] δ 10.06 (s, 2H), 7.55 (d, J = 8.52, 4H), 7.25 (d, J = 8.52 Hz, 4H), 3.46 (s, 2H) 3.43 (s, 8H), 2.87 (t, J = 5.02 Hz, 4H), 2.85 (t, J = 5.02, 4H). FABMS (m/z): Calc. for $C_{26}H_{33}N_5O_8S_2$: 608.21 $[MH]^+$. Found: 608.07 $[MH]^+$. Anal. Calc. for $C_{26}H_{33}N_5O_8S_2{\cdot}H_2O$: C, 49.91; H, 5.64; N, 11.19; S 10.25; Found: C, 50.47; H, 5.93; N, 11.23; S,10.56.

Synthesis of gadolinium(III) complex (GdL). To a solution of ligand (1.21 g, 2 mmol) in dry pyridine (10 mL) was added gadolinium(III) acetate tetrahydrate (0.81 g, 2 mmol). The suspension was stirred for 6 h at 70 °C during which time a yellow solution resulted. Solvent from the reaction mixture was stripped off and the residue was taken in ethanol (40 mL). The resulting solution was refluxed for 2 h. The solvent was removed and the residue taken up in ethanol (5 mL). The title complex was precipitated as a white solid by adding the ethanolic solution drop wise into acetone at 0 °C. The product was isolated by filtration, washed thoroughly with acetone, dried under vacuo at 60 °C for 8 h. Yield 0.74 g, (57.8%). FABMS (*m/z*): calcd for $C_{26}H_{32}GdN_5O_9S_2$, 781.12 ($[MH]^+$), $C_{34}H_{55}GdN_5O_{14}$, 763.23 $(MH\text{-}(H_2O))^+$; found, 781.17 ($[MH]^+$), 763.27 (MH-(H_2O)) Anal. Calcd for $C_{26}H_{32}GdN_5O_9S_2{\cdot}2.5H_2O$: C, 37.85; H, 4.52; N, 8.49; S, 7.76 Found: C, 38.34; H, 4.22; N, 8.96; S, 7.24.

Synthesis of GdL-unctionalized gold nanoparticles (GdL@Au). Citrate coated gold nanoparticles of size 12 nm were first prepared by the well established method that consisted of reducing $HAuCl_4$ with sodium citrate. In a 3L round bottom flask equipped with a condenser, $HAuCl_4{\cdot}3H_2O$ (0.33 g, 1 mmol in water (1 L) was brought to boil with vigorous stirring. Rapid addition of sodium citrate (1.14 g, 3.88 mmol) to the vortex of the solution resulted in a color change from yellow to purple. Boiling was continued for 10 min; the heating mantle was then removed, and the stirring was continued for another 10 min. The gadolinium complex coated AuNP was accomplished typically as follows: To a solution of AuNPs as prepared (1000 mL) GdL (1.5 g) was added and stirred for 20 h. An equal amount of acetone was added and the solution was further stirred for 4 h. The nanoparticles were collected by centrifugation and washed successively with water, acetone and ether.

XRD. XRD data were collected on Philips X-PERT X-ray diffractometer employing Cu Kα radiation (l = 1.5405 Å) at 40 kV and 25 mA. The diffraction pattern was acquired over a 2θ range between 20.02 and 89.99° with accounting time of 24.55 s per step.

TEM. One drop of aqueous GdL@Au solution was deposited on the copper carbon grid (200 mesh), and allowed to dry at room temperature. The sample was observed on a TEM (Philips CM200) operated at 200 kV.

ICP-MS. Determination of Au and Gd contents on GdL@Au was performed by ICP-MS analysis (Thermo Jarrell Ash ARIS-AP, USA). The sample was pre-treated and diluted with HNO_3 and HCl. Calibration curves were prepared for Au and Gd using standard solutions (ICP Element Standard solutions, Merck).

TGA. TGA was performed with a TG/DTA 320 & SSC 5200H Disk Station (Seiko) model on around 5 mg of dry, purified samples under an air flow of 40 mL min^{-1} at a heating rate of 10 °C min^{-1} in the temperature range of 0 - 800 °C.

***In vitro* CT.** Different concentrations of GdL@Au, Au@L, and iopromide-150 (Ultravist® 150 mg I/mL, Bayer HealthCare Pharmaceuticals) were prepared in 0.2 mL vials, and the vials placed in a custom-designed holder. CT was performed using an INVEON (Siemens Medical Solutions) CT scanner with 60 kVp, 500 μA, and 200-millisecond per frame. The reconstruction image size was 512 × 512 pixels. A uniform small region of interest was carefully placed over the center of each vial to measure attenuation values of fluid-filled vials containing GdL@Au L, L@Au, and Ultravist®.

Relaxivity measurements. T1 measurements were carried out using an inversion recovery method with a variable inversion time (TI) at 1.5 T (64 MHz). The magnetic resonance (MR) images were acquired at 35 different TI values ranging from 50 to 1750 msec. T1 relaxation times were obtained from the non-linear least square fit of the signal intensity measured at each TI value. For T2 measurements, the CPMG (Carr-Purcell-Meiboon-Gill) pulse sequence was adapted for multiple spin-echo measurements. Thirty four images were acquired with 34 different echo time (TE) values ranging from 10 to 1900 msec. T2 relaxation times were obtained from the non-linear least squares fit of the mean pixel values for the multiple spin-echo measurements at each echo time. Relaxivities (r1 and r2) were then calculated as an inverse of relaxation time per mM. The determined relaxation times (T1 and T2) and relaxivities (r1 and r2) were finally image-processed to give the relaxation time map and relaxivity map, respectively.

***In vitro* cell toxicity.** 14D Chick cornea epithelium primary cells (p1) were used. The cells obtained from Department of Biology, Kyungpook National University were grown in 100 cm^2 plastic culture dishes (Corning® Culture Dish) in 10 mL of medium at 37 °C under the atmosphere of CO_2 with 5% humidi-

ty. Cells were maintained in F-12-medium (Gibco®) supplemented with heat-inactivated 10% FCS, 1% chicken serum, 5 mg/mL insulin, 10 ng/mL human recombinant EGF, 100 IU/mL penicillin, 100 mg/mL streptomycin, and 200 mg/mL gentamicin (all purchased from Gibco®). The medium was replaced every 2 days, and cells split into a 96-well plate (2.5×10^4 cells/well/200 mL). Various gold concentrations (0.01 mM - 1.0 mM) of the contrast agent were added into the culture serum free media and incubated for 24 h. MTT (10 mL) was then added to each well to evaluate cell viability. The solution was removed after 4 h at 37 °C. The cells were dissolved in DMSO (100 mL), and the O. D. read at 560 nm using an ELISA (Molecular Device, USA Bio-rad 550 Reader) to determine the cell viability/toxicity.

Results and Discussion

Synthesis and characterization. The final product GdL@Au was prepared according to the method described elsewhere with a slight modification (Scheme 1).[11] The conjugate of DTPA-bis(amide) with 4-aminothiphenol (L) was prepared straightforwardly from the reaction of DTPA-bis(anhydride) with two equivalents of 4-aminothiphenol in DMF at 65 °C for 6 h. The subsequent reaction of with $Gd(OAc)_3$ in pyridine at 65 °C led to the formation of GdL as a white solid. The coating of AuNPs with GdL was accomplished by direct addition of an aqueous solution of GdL to a solution of citrate-coated AuNPs with a size of ~12 nm. Stirring was continued for 24 h before GdL@Au nanoparticles were collected by centrifugation and washed successively with water, acetone, and ether. The formation of GdL as $[Gd(L)(H_2O)]\cdot xH_2O$ and GdL@Au was confirmed by analytical and spectroscopic techniques. For instance, FAB-MS shows the molecular peak at 763 Da corresponding to $[M]^+ - H_2O$. Figure 1 shows the powder X-ray diffraction for Au@GdL. Namely, the peaks at 38.2°, 44.4°, 64.5°, 77.5°, and 81.7° correspond to the planes of (111), (200), (220), (311) and (222), respectively, the pattern of which is typical of Au NPs.[12] The TEM image in Figure 2 shows well-dispersed spherical particles of GdL@Au with the mean size of 12 nm. The visible absorption spectrum shows a band at ca. 540 nm corresponding to the excitation of surface Plasmon vibrations. This observation is consistent with that made with mono-dispersed gold nanoparticles of the same size.

GdL may bind to AuNPs in various modes as illustrated in Scheme 1 as thiols in GdL may undergo air-oxidation to form disulphide bonds. The same observation has also been reported with analogous Gd(DTDTPA)@Au.[9] The binding of GdL to the Au NP surface was confirmed by FT-IR and inductively coupled plasma mass spectrometry (ICP-MS). The S-H stretching band at 2368 cm^{-1} in GdL is absent in GdL@Au indicating the formation of Au-S bonds.[13-14] The concentration of gadolinium as well

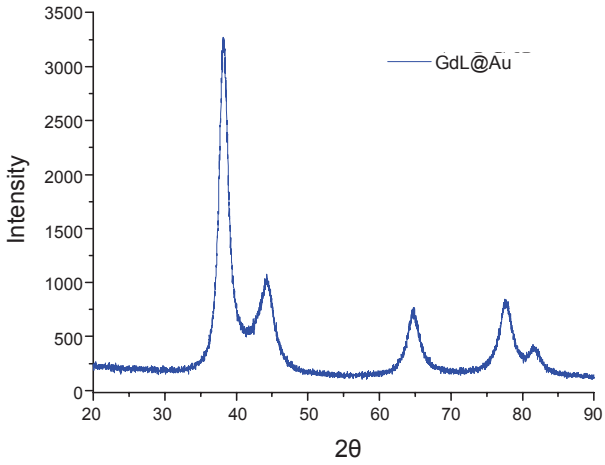

Figure 1. X-ray diffraction pattern of GdL@Au.

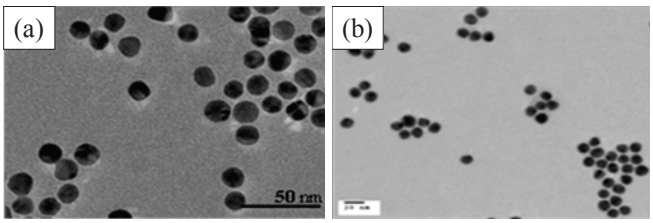

Figure 2. TEM images of (a) Citrated-coated gold nanoparticles and (b) Gadolinium chelate-coated gold nanoparticles.

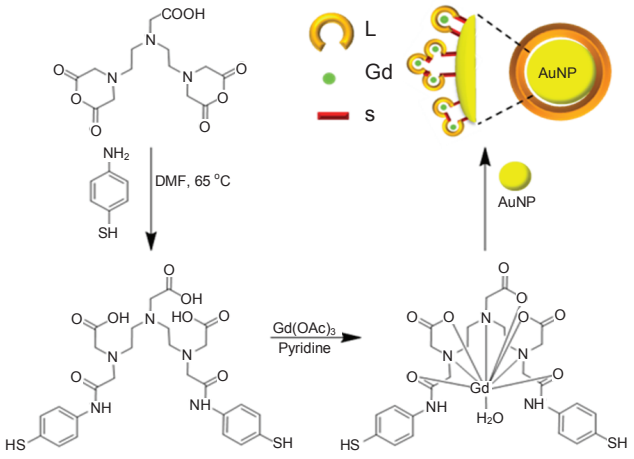

Scheme 1. Synthesis of GdL@Au

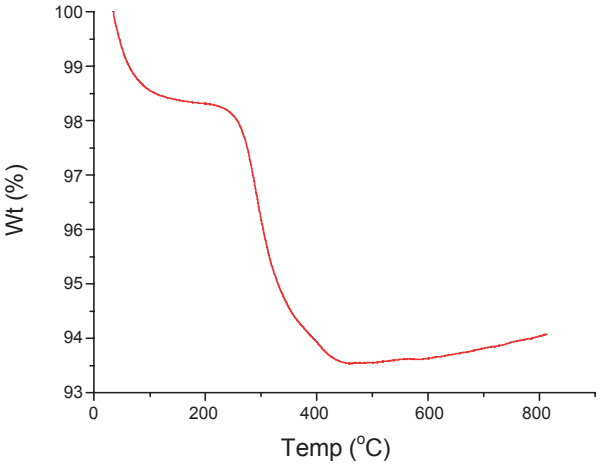

Figure 3. TGA curve of GdL@Au.

Table 1. Relaxivity data of GdL@Au

CA [mM]	$r1$($mM^{-1}s^{-1}$)	$r2$ ($mM^{-1}s^{-1}$)
Omniscan®	3.30 ± 0.02	3.70 ± 0.06
GdL	6.3 ± 0.04	9.2 ± 0.16
GdL@Au: [Gd]	10.0 ± 0.01	19.6 ± 0.56
GdL@Au: [AuNP]	1.4 × 104	2.7 × 104

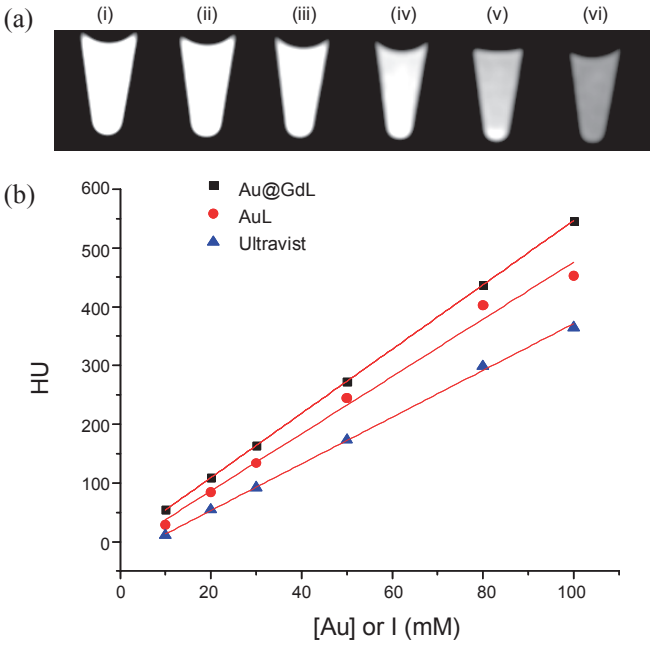

Figure 4. (A) CT phantom images at different concentrations: (i) 158.6 mM; (ii) 127.8 mM; (iii) 79.8 mM; (iv) 47.5 mM; (v) 31.7 mM and (vi) 15.8 mM. (B) CT plot showing the attennuation (in HU) for Ultravist, AuL and GdL@Au.

as the number of GdLs per AuNP was determined by inductively coupled plasma mass spectrometry (ICP-MS) for Gd and Au following the procedure reported earlier.[15] Namely, determination of the gold concentration followed by theoretical calculation based on the average size of 12 nm reveals the total number of GdLs per AuNP to be about 1.4×10^3. A further confirmation of such a high loading of GdL comes from the TGA results which show the weight loss of 4.7% in the temperature range 100 - 800 °C, corresponding to the decomposition of the organic ligand (Figure 3). This value matches well with the total number of GdLs per nanoparticle calculated based on the ICP data. Such a number of GdLs per AuNP is unusually high and almost 10-times as high as that found with Gd(DTDTPA)@Au.[9]

***In vitro* x-ray computed tomography.** To determine the potential usage of these NPs as CAs, *in vitro* X-ray absorption experiments were carried out in water. Figure 4 shows the phantom images and plots of *in vitro* X-ray attenuation of GdL@Au, L@Au, and Ultravist® as a function of concentration. As expected, both GdL@Au and L@Au exhibit higher attenuation than Ultravist®, a clinically used iodine-based CT CA; the differences become greater as the concentration increases.[16] At higher concentration of 100 mM [Au], the X-ray attenuation is

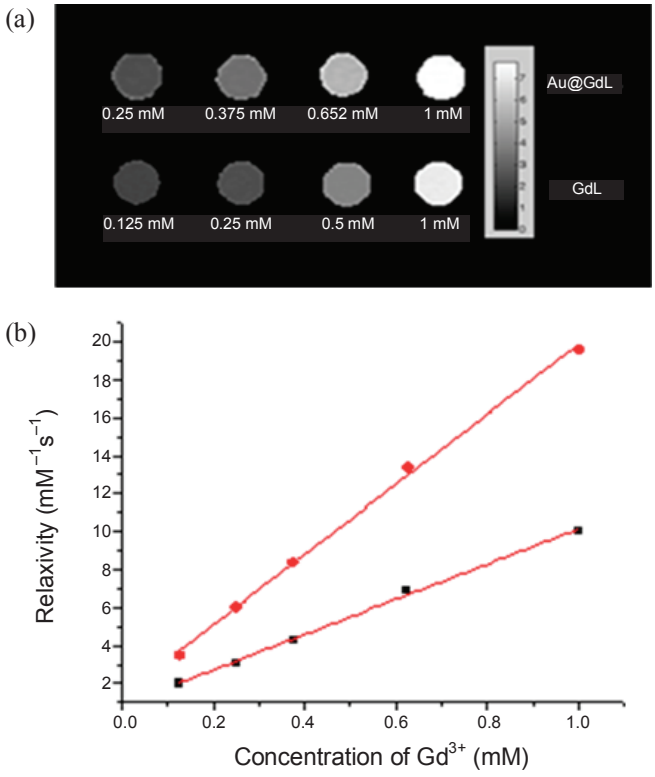

Figure 5. (a) $r1$ maps on GdL@Au and GdL (b) Plot of $r1$ and $r2$ as a function of gadolinium concentration in GdL@Au.

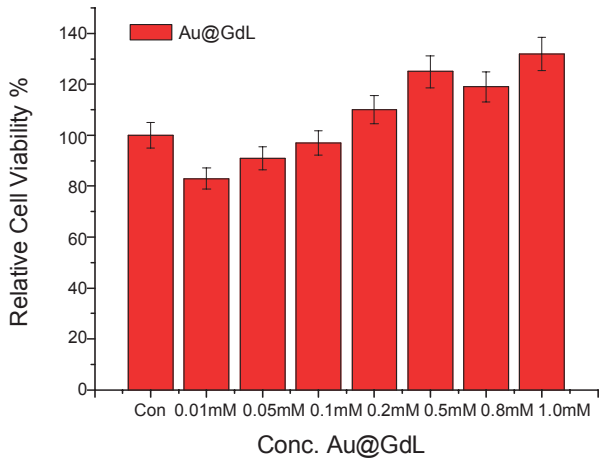

Figure 6. Relative cell viability (%) of the 14D Chick embryo cornea epithelial cells obtained with GdL@Au. The standard deviations (±SD) were obtained on a triplicate analysis (n = 3).

more due to the higher attenuation effect of Au leading to marked difference from the iodine-based contrast agents. This result clearly indicates that the GdL-coated AuNPs have a high potential for use in *in vivo* CT imaging. Although the gadolinium K-edge energy (50.2 keV) is largely lower than the one of gold, gadolinium ions immobilized on each nanoparticle ([Gd]) 2.6 mM for [Au]) 158.6 mM) seem to contribute to a small contrast enhancement of the CT images.

***In vitro* MRI.** Table 1 shows relaxivities ($r1$, $r2$) of Omniscan®, GdL and GdL@Au at the 1 mM concentration at 293 K and 1.5 T. GdL exhibits $r1$ relaxivity approximately twice higher than those of Omniscan®. These differences can be clearly observed by their $r1$ maps at varying concentrations shown in Figure 5a. Figure 5b shows the plots of $r1$ and $r2$ relaxivites of GdL@Au as a function of nanoparticle concentration, [Gd]. This system exhibits very high relaxivities ($r1 = 1.4 \times 10^4$ mM^{-1} s^{-1} and $r2 = 2.7 \times 10^4$ $mM^{-1}s^{-1}$) in terms of Au NP concentration. These values can be compared well with those of silica-based multilayered nanoparticles,[17] and compared even better with those of an analogous system.[9] Such high molecular relaxivities may be partially rationalized in terms of slower tumbling motion of GdL on AuNPs due to the formation of rigid oligomeric framework resulted from disulfide bonds (Scheme 1).

Cytotoxicity assay. The cytotoxicity assay was performed with GdL@Au as well as Omniscan® on 14D Chick cornea stroma primary cells. Figure 6 demonstrates that the cell proliferation and the viability are not affected when incubated for 24 h at various concentrations of GdL@Au. These observations indicate that GdL@Au has very low cytotoxicity and hence can be studied further for clinical usage. Relative cell viability (%) of the 14D Chick embryo cornea epithelial cells obtained with GdL@Au. The standard deviations (±SD) were obtained on a triplicate analysis ($n = 3$).

Conclusions

In summary, we have described the synthesis and characterization of Gold nanoparticles functionalized by Gd-complex of DTPA-bis(amide) conjugate of thiophenol as an MRI/CT bimodal contrast agent. The numbers of loading of GdL per gold nanoparticle are approximately 1.4×10^3. Our system shows extremely high $r1$ and $r2$ relaxivities in the order 10^4 $mM^{-1}s^{-1}$. A synergistic effect of gadolinium in GdL@Au on X-ray attenuation has been observed. These nanoparticles exhibit low cytotoxicity, showing their further practical applicability.

Acknowledgments. T.-J.K. gratefully acknowledges the KRF for financial support (Grant No. C00438). NMR and mass spectral measurements were performed by the KBSI.

References

1. For comprehensive recent reviews, see: a) Caravan, P. *Chem. Soc. Rev*. **2006**, *35*, 512. b) Caravan, P.; Ellison, J. J.; McMurry, T. J.; Lauffer, R. B. *Chem. Rev*. **1999**, *99*, 2293. c) Aime, S.; Botta, M.; Fasano, M.; Terrono, E. *Chem. Soc. Rev*. **1998**, *27*, 19. d) Hermann, P.; Kotek, J.; Kubicek, V.; Lukes, I. *Dalton Trans.* **2008**, 3027.
2. Merbach, A. E.; Tóth, É. *The Chemistry of Contrast Agents in Medical Magnetic Resonance Imaging*; John Wiley & Sons, Ltd: Chichester, UK, 2001.
3. a) Crch, S. G.; Bussolati, B.; Tei, L.; Grange, C.; Esposito, G.; Lanzardo, E.; Camussi, G.; Aime, S. *Cancer Res.* **2006**, *66*, 9196. b) Sitharaman, B. Kissell, K. R.; Hartman, K. B.; Tran, L. A.; Baikalov, A.; Rusakova, I.; Sun, Y.; Khant, H. A.; Ludtke, S. J.; Chiu, W.; Laus, S.; Tóth, Ë.; Helm, L.; Merbach, E.; Wilson, L. J. *Chem. Commun*. **2005**, 3915. c) Aime, S.; Botta, M.; Fasano, M.; Genimatti Crich, S.; Terreno, E. *Coord. Chem. Rev*. **1999**, *321*, 185. d) Aime, S.; Frullano, L.; Crish, S. G. *Angew. Chem. Int. Ed.* **2002**, *41*, 1017. e) Reynolds, C. H.; Annan, N.; Beshah, K.; Huberm, J. H.; Shaber, S. H.; Lenkinski, R. E.; Wortman, J. A. *J. Am. Chem. Soc*. **2000**, *122*, 8940. f) Aime, S.; Cabella, C.; Colombatto, S.; Crich, S. G.; Gianolio, E.; Maggioni, F. *J. Magn. Res. Imaging*. **2002**, *16*, 394.
4. Sanchez, P.; Valero, E.; Galvez, N.; Domminguez-Vera, J. M.; Marinone, M.; Poletti, G.; Corti, M.; Lascialfari, A. *Dalton Trans.* **2009**, 800.
5. a) Kircher, M. F.; Mahmood, U.; King, R. S.; Weissleder, R.; Josephson, L. *Cancer Res.* **2003**, *63*, 8122. b) Devaraj, N. K.; Keliher, E. J.; Thurber, G. M.; Nahrendorf, M.; Weissleder, R. *Bionconjugate Chem.* **2009**, *20*, 397. d) Kim, J.; Kim, H. S.; Lee, N.; Kim, T.; Kim, H.; Yu, T. ; Song, I. C.; Moon, W. K.; Hyeon, T. *Angew. Chem.* **2008**, *47*, 1.
6. a) Hu, K. W.; Jhang, F. Y.; Su, C. H.; Yeh, C. S. *J. Mat. Chem*. **2009**, *19*, 2147. b) Lim, Y. T.; Cho, M. Y.; Choi, B. S.; Lee, J. M.; Chung, B. H. *Chem. Commun*. **2008**, 4930.
7. Fenchel, S.; Fleiter, T. R., Aschoffm A. J.; Gessel, R. V.; Brambs, H. J.; Merkle, E. M. *Br. J. Radiol*. **2004**, *77*, 821. b) Enicina, J. L.; Bonmati, L. M.; R-Oms, C. L.; Rodriguez, V. *Eur. Radiol*. **1997**, *7*, S115.
8. Hainfeld, J. F.; Slatkin, D. N.; Focella, T. M.; Smilowitz, H. M.; *Br. J. Radiol*. **2006**, *79*, 248. b) Kattumuri, V.; Katti, K.; Bhaskaran, S.; Boote, E. J.; Casteel, S. W.; Fent, G. M; Robertson, D. J.; Chandrasekhar, M.; Kannanm R.; Katti, K. V. *Small* **2007**, *3*, 333. c) Cai, Q. U.; Kim, S. H., Choi, K. S.; Kim, S. Y., Byun, S. J.; Kim, K. W.; Park, S. H.; Juhng, S. K.; Yoon, K. H. *Invest Radiol*. **2007**, *42*, 797.
9. a) Debouttiere, P. J.; Roux, S.; Vocanson, F.; Bilotey, C.; Beuf, O.; Favre-Reguillon, A.; Lin, Y.; Pellet-Rostaing, S.; Lamartine, R.; Perriat, P.; Tillement, O. *Adv. Funct. Mater*. **2006**, *16*, 2330. b) Alric, C.; Taleb, J.; Duc, G. L.; Mandon, C.; Bilotey, C.; Meur-Herland, A. L.; Brochard, T.; Vocanson, F.; Janier, M.; Perriat, P.; Roux, S.; Tillement, O. *J. Am. Chem. Soc*. **2008**, *130*, 5908.
10. a) Dutta, S.; Kim, S. K.; Patel, D. B.; Kim, T. J.; Chang, Y. M. Polyhedron **2007**, *26*, 3799. b) Dutta, S.; Park, J. A.; Jung, J. C.; Chang, Y. M.; Kim, T. J. *Dalton Trans*. **2008**, *16*, 2199. c) Park, J. A.; Lee, J. J.; Jung, J. C.; Yu, D. Y.; Oh, C.; Ha, S.; Kim, T. J.; Chang, Y. M.; *ChemBioChem*. **2008**, *9*, 2811. d) Park, J. A.; Reddy, P. A. N.; Kim, H. K.; Kim, I. S.; Kim, G. C.; Chang, Y.; Kim, T. J. *Bioorg. Med. Chem. Lett*. **2008**, *18*, 6135.
11. Grabar, K. C.; Freeman, R. G.; Hommer, M. B.; Natan, M. J. *Anal. Chem.* **1995**, *67*, 735.
12. Joing Committee of powder diffraction Standard (JCPDS) Card No. 04-0784, **2002**.
13. Yonezawa, T.; Kunitake, T. *Coll. Surf. A* **1999**, *149*, 193.
14. Daniel, M. C.; Astruc, D. *Chem, Rev*. **2004**, *104*, 293.
15. Kim. J. S.; Rieter, W. J.; Taylor, K. M. L.; An, H.; Lin, W. *J. Am. Chem. Soc*. **2007**, *129*, 8962.
16. Riester, W. J.; Kim, J. S.; Taylor, K. M. L.; An, H.; Lin, W; Tarrant, T. *Angew. Chem. Int. Ed*. **2007**, *46*, 3680.
17. Alric, C.; Taleb, J.; Duc, G. L.; Mandon, C.; Bilotey, C.; Meur-Herland, A. L.; Brochard, T.; Vocanson, F.; Janier, M.; Perriat, P.; Roux, S.; Tilement, O. *J. Am. Chem. Soc.* **2008**, *130*, 5908.